Electronic Supporting Information for The limit of macroscopic homogeneous ice nucleation at the nanoscale

John A. Hayton,[1] Michael B. Davies,[2,1] Thomas F. Whale,[3,4] Angelos Michaelides,[1] and Stephen J. Cox[1]

[1)] *Yusuf Hamied Department of Chemistry, University of Cambridge, Lensfield Road, Cambridge CB2 1EW, United Kingdom*

[2)] *Department of Physics and Astronomy, University College London, London WC1E 6BT, United Kingdom*

[3)] *Department of Chemistry, University of Warwick, Gibbet Hill Road, Coventry CV4 7AL, United Kingdom.*

[4)] *School of Earth and Environment, University of Leeds, Woodhouse, Leeds LS2 9JT, United Kingdom*

(Dated: 2 October 2023)

This document includes: methodology for all simulations in the main paper; a sensitivity analysis of the nucleation rate to $\Delta\mu$; committor distributions for 2.5 nm and 5 nm films; density profiles for the physically confined films; volumetric nucleation rates obtained by seeding and cooling ramps compared to literature values; and preliminary work using seeding comparing bulk to film samples in TIP4P/ice[(8.5)].

I. METHODOLOGY

All simulations were performed with LAMMPS,[1] with particle positions propagated with the velocity verlet algorithm.[2] The timestep, δt, was set at 10 fs in mW simulations and 2 fs in TIP4P/ice$^{(8.5)}$ simulations. Simulations of thin water films employed a slab geometry under periodic boundary conditions, with the temperature maintained with a Nosé-Hoover thermostat with a damping constant $100\delta t$. Simulations of bulk water were performed under periodic conditions in the NPT ensemble; temperature was similarly maintained with a Nosé-Hoover thermostat,[3] and pressure maintained at 0 bar with a Parinello-Rahman barostat[4] with damping constant $1000\delta t$.

A. Preparation of thin mW films

For unsupported thin films, the thickness W was defined as

$$W = N/A\bar{\rho} \tag{S1}$$

with N the number of molecules, A the cross sectional area of the film, and $\bar{\rho} = 33.3774\,\mathrm{nm}^{-3}$ the bulk density of mW molecules at 220 K. By running initial tests at 6000 and 8192 molecules in the 6 nm film, we found that there were no significant finite size effects present for a critical seed in a 6000 particle system, akin to previous investigations that selected similar sized lateral dimensions.[5,6] W was therefore controlled by selecting the x and y dimensions (l_x and l_y respectively) of the film so that $l_x = l_y = \sqrt{N/W\bar{\rho}} = 13.40\,\mathrm{nm} \times \sqrt{1\,\mathrm{nm}/W}$.

To generate an initial configuration of mW water molecules for a given film width, the packmol software[7] was used to randomly pack 6000 mW particles in a cuboid between $(0,\, 0,\, -W/2)$ and $(l_x,\, l_y,\, W/2)$. The z dimension (l_z) of the simulation box was then increased by a factor of 3 to generate a liquid-vapor interface. The films were equilibrated at 220 K for 10000 steps at timesteps of 0.1 fs, 0.5 fs, 1 fs, 2 fs and 5 fs sequentially, before further equilibration for 50000 steps at a 10 fs timestep. After this, the systems were judged to have equilibrated, as the density of the center of the film and enthalpy had converged.

Independent initial configurations of the mW films were generated by performing simulations of the equilibrated film at 220 K and taking the positions of all atoms every 100 ps.

B. Preparation of bulk mW systems

An initial random configuration of mW particles was generated using packmol, with $l_x = l_y = l_z = (N/\bar{\rho})^{1/3}$. The system was then equilibrated with the protocol described in Sec. I A, with the density and enthalpy adjudged to have equilibrated. Independent configurations were then sampled as described in Sec. I A

C. Preparation and simulation of mW seeding systems

Independent configurations of mW as hexagonal ice were generated by first utilizing the GenIce package to create an initial configuration of TIP4P/ice molecules in the ice Ih crystal structure. The hydrogens were stripped out using python code, and the oxygens relabeled as mW particles, to generate a system of mW particles in the Ih crystal structure with $N = 16000$. The system was allowed to equilibrate at 220 K and 0 bar for 10 ns. Independent configurations were then obtained by allowing the system to further evolve at 220 K and 0 bar, with the positions of all molecules taken every 100 ps.

To generate seeding systems, an initial configuration of mW particles of the desired system (i.e., thin film or bulk liquid) is selected, and python code utilizing the MDAnalysis software package[8,9] is used to cut a spherical cavity in the liquid. A spherical cluster of Ih is created by cutting a similar sphere out of an initial configuration of ice Ih. The spherical seed is placed in the cavity cut in the liquid configuration to initialize a seeding system.

Seeding systems progressed by first allowing the liquid molecules to equilibrate for 80 ps at 220 K with the molecules in the seed held fixed; for a seed immersed in the bulk liquid, pressure was also maintained at 0 bar. This was done to allow a more realistic liquid/crystal interface to develop, with 80 ps selected to allow enough time for this surface to relax, but not so long that the seeds close to the critical size grew substantially. Then, all particles were allowed to evolve until either $n_{\mathrm{cl}} \gg n_{\mathrm{cl}}^{\ddagger}$ (taken as $n_{\mathrm{cl}} \geq 400$) or $n_{\mathrm{cl}} \approx 0$ (taken as $n_{\mathrm{cl}} \leq 20$). Information on how the n_{cl} was identified and monitored is given in Sec. II.

D. Obtaining $n_{\mathrm{cl}}^{\ddagger}$ and f^{+} from seeding simulations

The probability of growth, $p_{\mathrm{ice}}(n_{\mathrm{cl}}^{*}; W)$ for a given cluster size n_{cl}^{*} is found by considering all initial clusters of size $n_{\mathrm{cl}}^{*} - 9 \leq n_{\mathrm{cl}}(t = 0) \leq n_{\mathrm{cl}}^{*} + 9$. The probability of growth for this

group of simulations was found as $p_{\rm ice}(n^*_{\rm cl};W) = n(\text{Grown})/n(\text{Total})$. The bin size of 19 was selected as clusters were regularly observed to change size by ~ 9 molecules between frames in analysis, and corresponded to a 5% change in radius between the largest and smallest extremes of the range at criticality. $p_{\rm ice}(n^*_{\rm cl};W)$ was identified for all integer $n^*_{\rm cl}$, and combined to generate Fig. 3a. $p_{\rm ice}(n_{\rm cl};W) = 0.5$ was then identified to find $n^\ddagger_{\rm cl}$. The ranges presented as in Tab. 1. were found by splitting the entire data set (for each system) randomly into three subsets and repeating the analysis with each subset. The largest and smallest values obtained were quoted as the range.

Once $n^\ddagger_{\rm cl}$ was identified, the attachment rate as found by identifying all simulations for a given film width of initial cluster size $n^\ddagger_{\rm cl}-5 \leq n_{\rm cl}(t=0) \leq n^\ddagger_{\rm cl}+5$, and initiating simulations from these configurations. $\langle (n_{\rm cl}(t)-n^\ddagger_{\rm cl})^2 \rangle$ was found by assuming $n_{\rm cl}(t=0) \approx n^\ddagger_{\rm cl}$ and taking the average from all simulations. f^+ was then found by applying a linear fit, and taking half the gradient.

E. Preparation of TIP4P/ice systems

All simulations of TIP4P/ice were performed in a similar manner to their corresponding mW simulation, with electrostatic interactions computed with a particle-particle particle-mesh Ewald method,[10] with parameters chosen such that the root mean square error in the forces were a factor 10^5 smaller than the force between two unit charges separated by a distance of 1 Å.[11] For simulations of liquid water in contact with its vapor, we set the electric displacement field (along z) $D = 0$, using the implementation given in Refs. 12,13. The rigid geometry of the molecules was maintained with the RATTLE algorithm.[14]

TIP4P/ice systems were generated using a similar methodology to mW. The only film generated was made to match the film considered in Ref. 15, which had $N = 3072$ and $l_x = l_y = 4.8096\,\text{nm}$. Given the bulk density of TIP4P/ice[(8.5)] at 230 K was measured in this study as $\bar{\rho} = 30.9366\,\text{nm}^{-3}$, this gives $W = 4.3\,\text{nm}$. Similar to mW, the film was generated by creating an initial random configuration of TIP4P/ice molecules with packmol, before allowing the system to equilibrate. The bulk system was also generated to match Ref. 15, with $N = 4096$. It was generated and equilibrated in a manner similar to Sec. I B, but with the relevant fixes described above. In addition, to facilitate equilibration at this low temperature, we used replica exchange with temperature 230, 236, 242, 248 and 254 K; swaps

between replicas were attempted every 1 ps.[16,17]

F. Simulations with cooling ramps

Cooling ramp simulations were performed for $W = \infty$, 6.0 nm, 3.5 nm. The initial configurations generated in Secs. I A, I B were taken, and were cooled at a rate of $0.2\,\mathrm{K\,ns^{-1}}$ using a Nosé-Hoover thermostat with damping parameter 1000 fs. The systems were monitored every 100 ps, and the system was adjudged to be frozen when $n_{\mathrm{cl}} \geq 200$. In the rare case that a system recrossed 200 molecules, the later temperature at which n_{cl} passed 200 molecules was taken as the freezing temperature. Information on how the n_{cl} was identified and monitored is given in Sec. II.

G. Preparation of systems with physical confining boundaries

mW films were confined between the (111) face of a Lennard-Jones crystal, with parameters described in Tab. S1. This surface had been previously investigated by Davies *et al.*,[18] and shown to nucleate ice only for temperatures $T < 201\,\mathrm{K}$, significantly below the temperature of 220 K used for the seeding investigations performed in this study.

Parameter	Value
ϵ	$0.23\ \mathrm{kcal\,mol^{-1}}$
σ	2.5233 Å
LJ Cutoff	7.53 Å
Lattice Constant	4.1564 Å

TABLE S1. Parameters for the LJ crystal used to confine the thin film. This crystal face is shown to only nucleate ice below 201 K,[18] and so we consider it nucleation inactive for this study, with any nucleation events occurring at 220 K expected to happen far from the interface

1920 Lennard-Jones atoms were packed into a close-packed layer, and 5 such layers were combined to generate an FCC crystal with its close-packed face exposed, perpendicular to the z axis. This resulted in a crystal structure with dimensions $5.5778\,\mathrm{nm} \times 24.4336\,\mathrm{nm} \times$

1.1950 nm. This crystal was placed in a simulation cell with its uppermost layer at a position $z = -H/2$. An identical structure was placed with its lowermost layer at $z = H/2$.

Between these two layers, packmol was used to generate a random configuration of $N(H)$ mW molecules in a cuboid between $(0,\, 0,\, -H/2)$ and $(5.5778\,\mathrm{nm},\, 8\,\mathrm{nm},\, H/2)$. $N(H) = 1570 \times \frac{H}{[1\,\mathrm{nm}]}$ was selected so that the physically confined film spanned the x dimension of the LJ crystal, and approximately $1/3$ of the y.

The system was then allowed to equilibrate, and independent initial configurations sampled, in a manner similar to Sec. I A. Seeding systems were the generated and investigated in a manner similar to Sec. I C. The critical nucleus size was identified in a manner identical to Sec. I D.

The particles that make up the LJ crystal were not included in the dynamics, and did not contribute towards the simulation beyond their interaction with the mW particles.

II. ORDER PARAMETERS USED FOR IDENTIFYING CLUSTER SIZES

Clusters of ice-like particles were identified by first classifying each particle in the system as either liquid-like or crystal like, using the Steinhardt parameters defined in the main paper:

$$\bar{Q}_6^{(i)} = \frac{Q_6^{(i)} + \sum_j{}' Q_6^{(j)}}{\nu^{(i)} + 1}, \tag{S2}$$

with $Q_6^{(i)}$ defined with the 6$^{\text{th}}$ order spherical harmonics:

$$Q_6^{(i)} = \frac{1}{\nu^{(i)}} \sqrt{\sum_{m=-6}^{6} \sum_{j,k}{}' Y_{6m}^*(\hat{\mathbf{r}}_{ij}) Y_{6m}(\hat{\mathbf{r}}_{ik})}, \tag{S3}$$

For all mW simulations, particle j was considered adjacent (and so included in the summation of Eqns. S2 and S3) if the distance between particles i and j $|\mathbf{r}_{ij}| \leq 3.5\,\text{Å}$. For this we used the implementation in Plumed,[19,20] with the switching function $\sigma(|\mathbf{r}_{ij}|)$:

$$\sigma(|\mathbf{r}_{ij}|) = \begin{cases} 1 & \text{if } |\mathbf{r}_{ij}| \leq 3.5\,\text{Å} \\ \exp\left(-\frac{(|\mathbf{r}_{ij}| - 3.5\,\text{Å})^2}{2\times(0.05\,\text{Å})}\right) & \text{if } 3.5\,\text{Å} \leq |\mathbf{r}_{ij}| < 3.51\,\text{Å} \\ 0 & \text{if } 3.51\,\text{Å} \leq |\mathbf{r}_{ij}| \end{cases} \tag{S4}$$

This switching function leads to the selection of the $\nu^{(i)}$ nearest atoms to particle i, where $\nu^{(i)}$ is defined as

$$\nu^{(i)} = \sum_{j \neq i} \sigma(|\mathbf{r}_{ij}|) \tag{S5}$$

for all j mW particles in the system.

Once $\bar{Q}_6^{(i)}$ is identified for each mW particle i in the system, particles were identified as being ice-like or liquid-like through the use of a cutoff value $\bar{Q}_{6\text{C}} = 0.4021$. $\bar{Q}_{6\text{C}}$ was found by obtaining the probability distributions $P(\bar{Q}_6^{(i)})$ for both liquid mW and hexagonal ice mW at 220 K and 0 bar,[21] shown in Fig. S1. $\bar{Q}_{6\text{C}}$ was found as the value for which an equal proportion of Ih and liquid particles are misidentified.[22,23]

$$\int_0^{\bar{Q}_{6\text{C}}} P(\bar{Q}_{6,\,\text{Hex}}^{(i)}) d\bar{Q}_{6,\,\text{Hex}}^{(i)} = \int_{\bar{Q}_{6\text{C}}}^{1} P(\bar{Q}_{6,\,\text{Liq}}^{(i)}) d\bar{Q}_{6,\,\text{Liq}}^{(i)} \tag{S6}$$

Once all particles have been classified as liquid-like or crystal-like, the largest cluster of adjacent crystal-like particles is identified, using a depth-first clustering search and identifying particles i and j as adjacent if $|\mathbf{r}_{ij}| \leq 3.5\,\text{Å}$. The number of molecules of this cluster

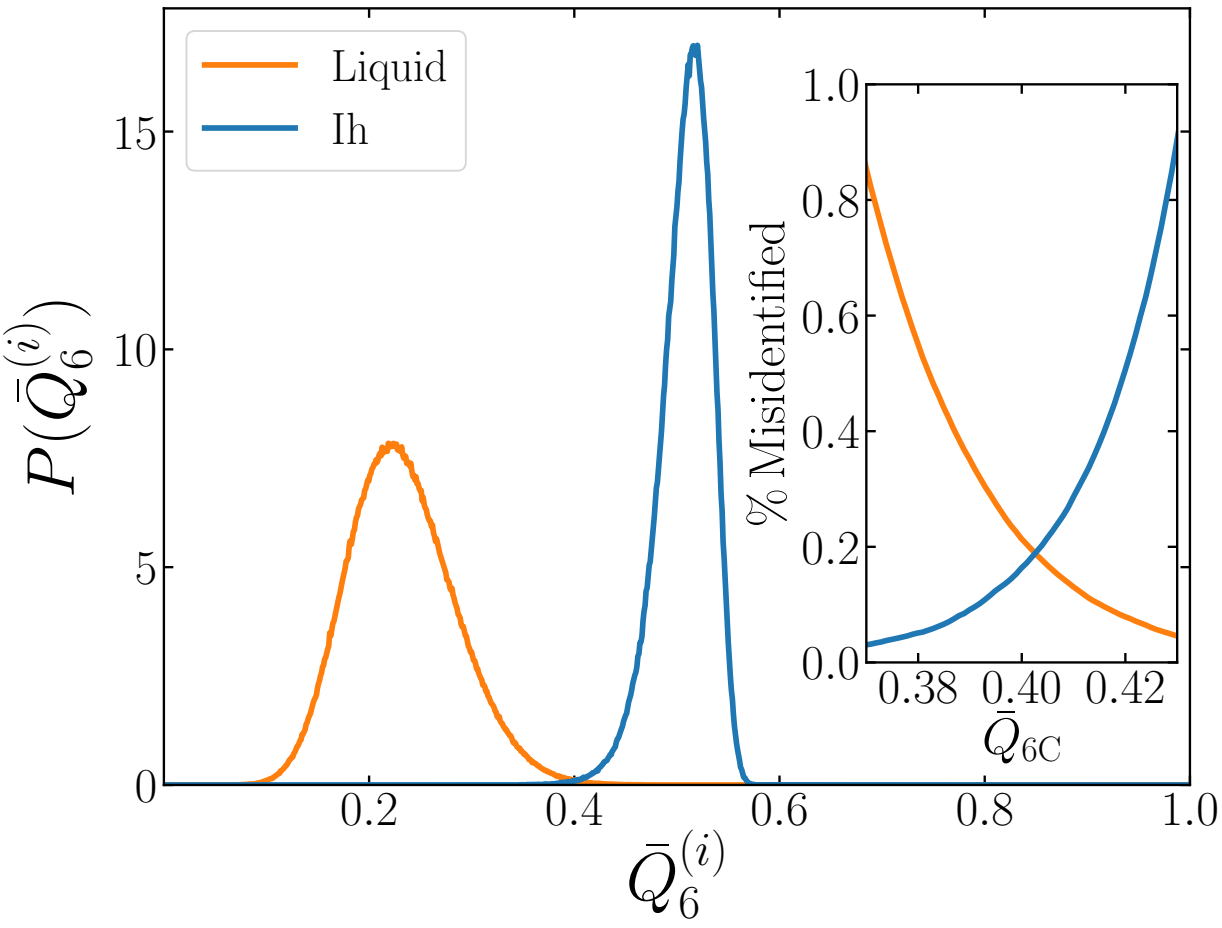

FIG. S1. $P(\bar{Q}_6^{(i)})$ for both liquid and hexagonal ice. Inset: The left hand side (blue) and right hand side (orange) of Eqn. S6 shown as a function of $P(\bar{Q}_{6C})$.

is taken as n_{cl}. Performing a similar analysis for TIP4P/ice at 230 K (with $|\mathbf{r}_{ij}|$ the distance between oxygen atoms on molecules i and j etc) gives $\bar{Q}_{6C} = 0.3946$.

III. SENSITIVITY OF THE NUCLEATION RATE FROM SEEDING TO $\Delta\mu$

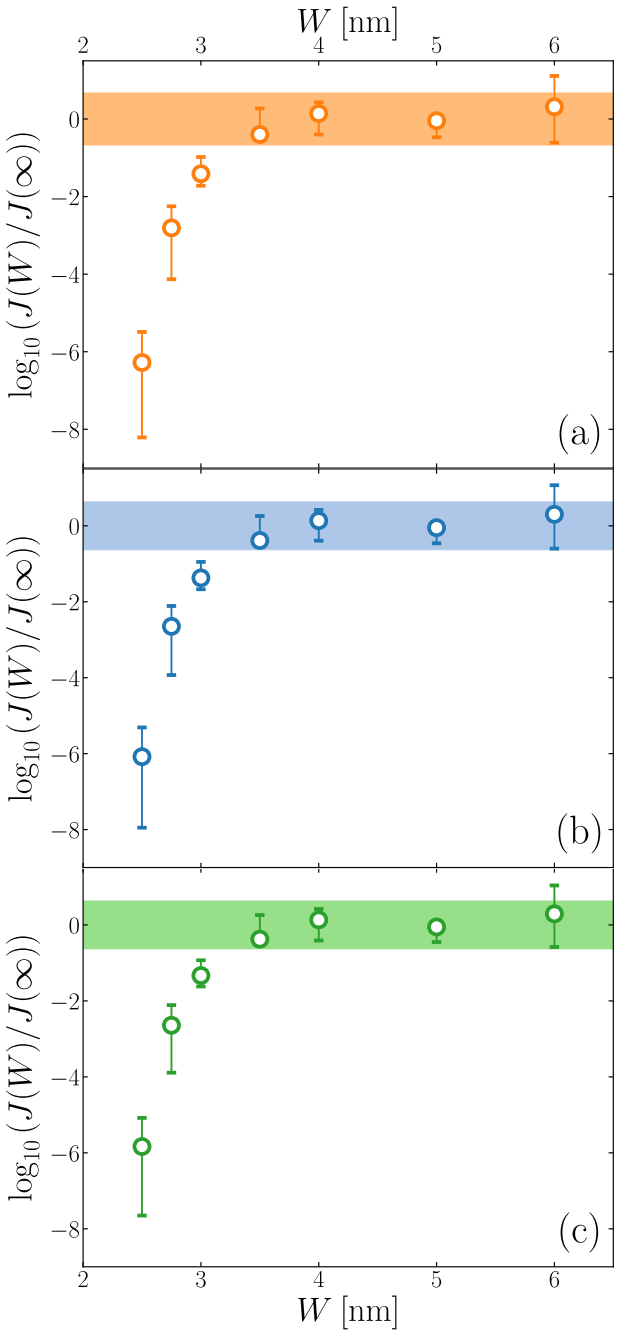

FIG. S2. $J(W)$ obtained with (a) $|\Delta\mu|/k_{\mathrm{B}} = 126\,\mathrm{K}$, (b) $|\Delta\mu|/k_{\mathrm{B}} = 122\,\mathrm{K}$ (same as Fig. 3d in the main text), and (c) $|\Delta\mu|/k_{\mathrm{B}} = 118\,\mathrm{K}$. The results are virtually indistinguishable from each other.

IV. COMMITTOR DISTRIBUTIONS OF 2.5 nm AND 5 nm FILMS

To test the suitability of n_{cl} as the "reaction coordinate", we present the committor distribution for n_{cl}. The committor distribution was found by first selecting clusters for which $n_{\mathrm{cl}}(t = 0) \approx n_{\mathrm{cl}}^{\ddagger}$ (taken in this case as $n_{\mathrm{cl}}(t = 0) = n_{\mathrm{cl}}^{\ddagger} \pm 3$). This resulted in 72 initial clusters for $W = 2.5\,\mathrm{nm}$ and 53 for $W = 5\,\mathrm{nm}$. For each cluster, 20 different simulations were performed where the velocities of each particle was randomized to create the expected velocity distribution at 220 K, and allowed to evolve until the seed grew or shrank. The probability $P(p_{\mathrm{B}})$ that a given cluster would grow to encompass the entire system is presented below.

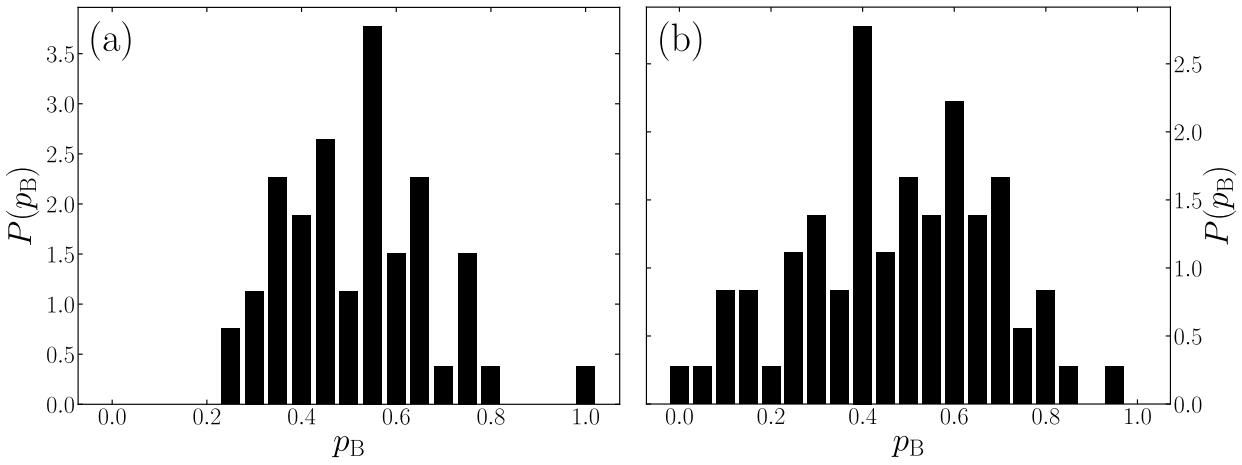

FIG. S3. Committor distributions for (a) 5 nm and (b) 2.5 nm films.

V. DENSITY PROFILES FOR DIFFERENT VALUES OF H

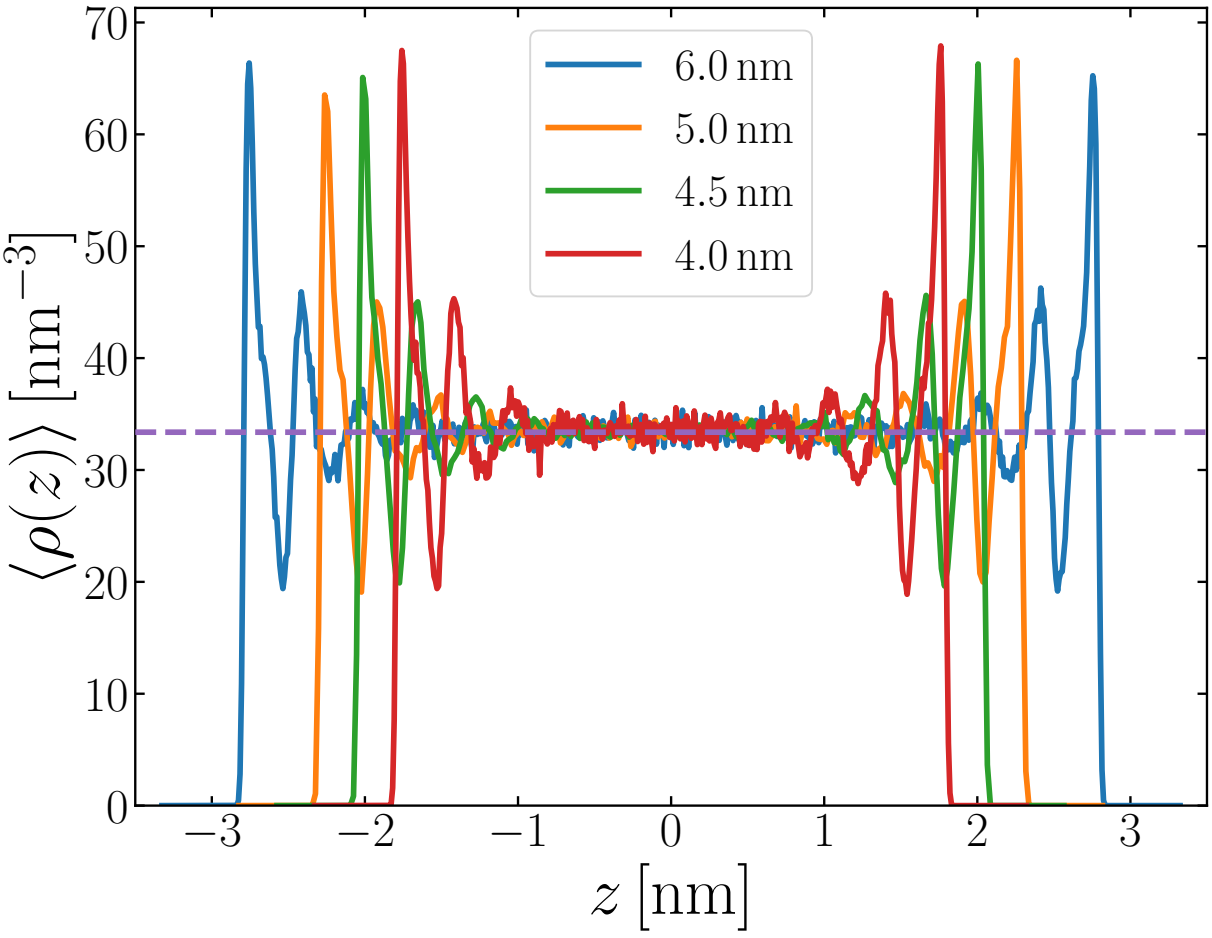

FIG. S4. $\langle \rho(z) \rangle$ for $H = 6.0\,\text{nm}$, $H = 5.0\,\text{nm}$, $H = 4.5\,\text{nm}$, $H = 4.0\,\text{nm}$. $\bar{\rho} = 33.3774\,\text{nm}^{-3}$, the bulk density for mW at 220 K and 0 bar, is included as the dashed line.

VI. VOLUMETRIC NUCLEATION RATES OBTAINED FROM COOLING RAMPS

Volumetric nucleation rates for the cooling ramps investigation, found by dividing the freezing rates of the bulk system by the Nv where $N = 6000$ is the number of molecules in the system, and $v = 3 \times 10^{-29}\,\mathrm{m}^{-3}$ is the volume of a single mW molecule under these conditions. These results are compared to previous literature values.[24–27]

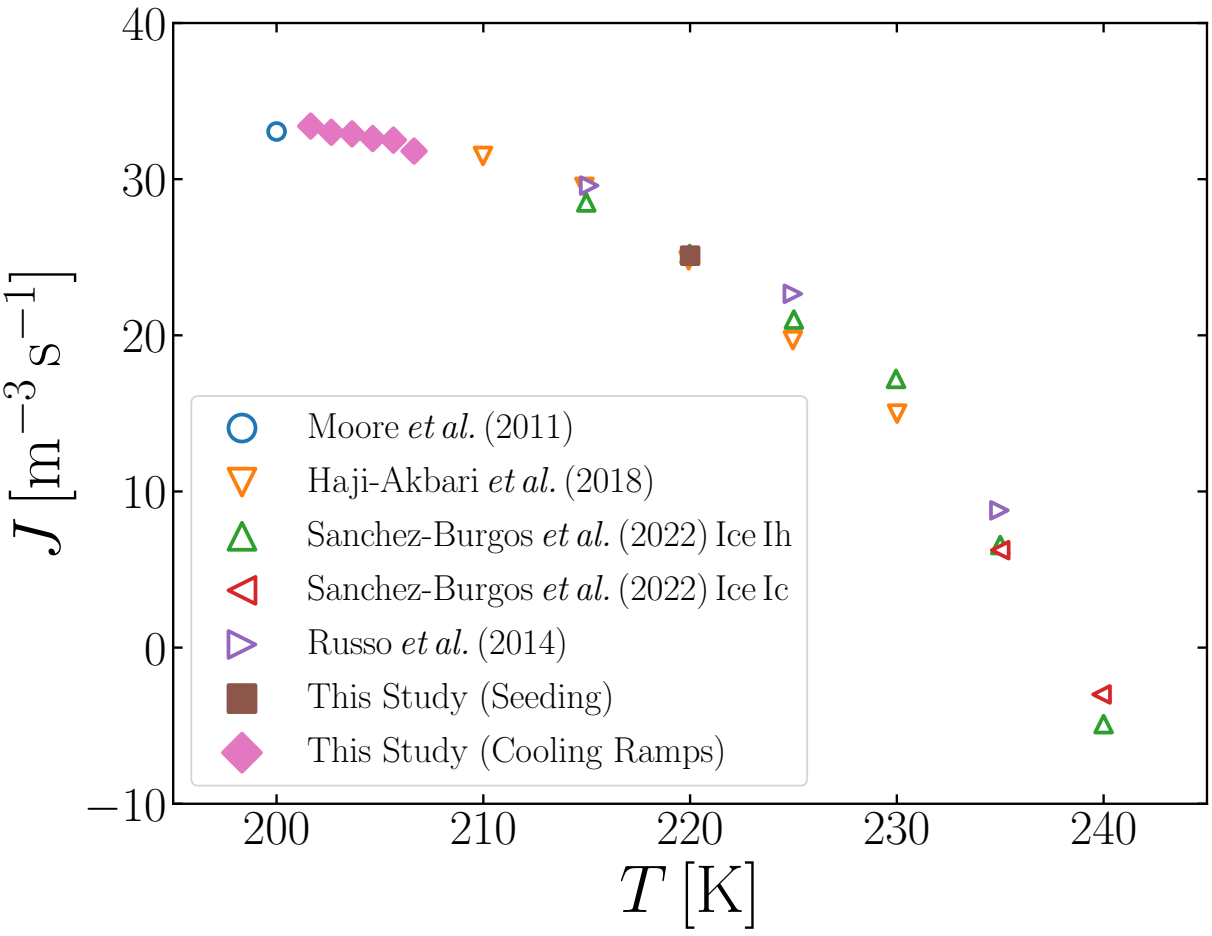

FIG. S5. $J(\infty)$ for this work and a range of previous studies.

VII. PRELIMINARY WORK ON TIP4P/ICE FILMS

We argue in the main paper that mW is suitable for this study, due to the mechanisms of ice formation being similar to TIP4P/ice[8.5], and similar convergence of structural order to bulk-like values within $\sim 1\,\mathrm{nm}$ from the surface. In this section, we present preliminary work using the TIP4P/ice[8.5] model for both bulk and film ($W = 4.3\,\mathrm{nm}$). Seeding was implemented in a manner similar to Sec. I C, but at 230 K and a 200 ps equilibration time instead of 80 ps. Additionally, the same method was used to identify ice-like molecules, with the oxygen in each molecule acting as the point which $\mathbf{r}_{ij}$ vectors point to and from. Due to the different conditions and model, $\bar{Q}_{6\mathrm{C}} = 0.3946$.

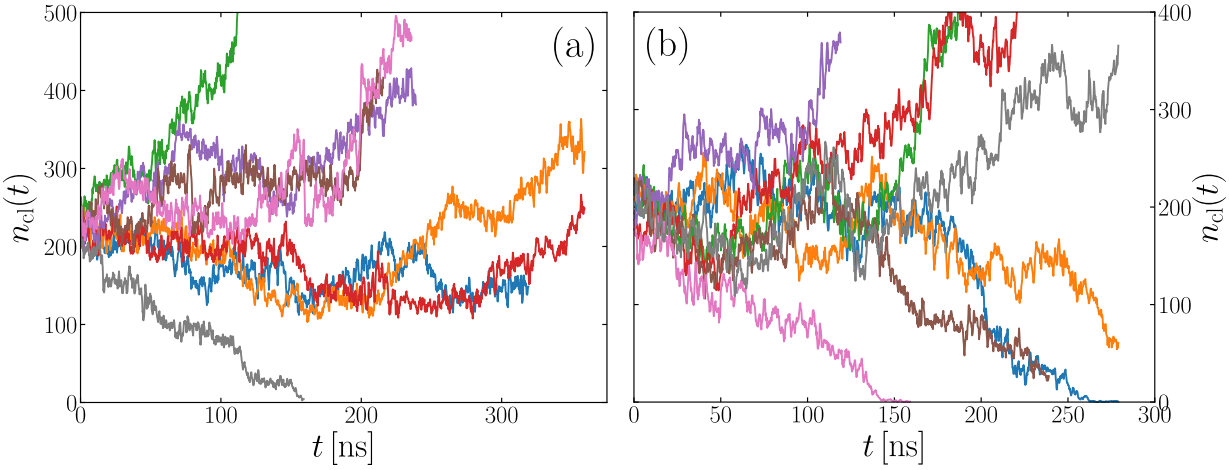

FIG. S6. $n_{\mathrm{cl}}(t)$ for 8 independent seeding simulations in a) a bulk system, $\langle n_{\mathrm{cl}}(t=0)\rangle = 232$ and b) a 4 nm film $\langle n_{\mathrm{cl}}(t=0)\rangle = 200$. In both cases, clusters of similar initial size grow and shrink, and some clusters spend significant time at or around their initial sizes. Both facts indicate these systems are at or near criticality.

This investigation was extremely limited in scope due to the high computational cost of TIP4P/ice[8.5]. However, we show that both film and bulk appear to be near critical for $n_{\mathrm{cl}}(t=0) \approx 200$. The fact that bulk and film systems appear to report similar critical nuclei further supports our mW-based study.

REFERENCES

[1]A. P. Thompson, H. M. Aktulga, R. Berger, D. S. Bolintineanu, W. M. Brown, P. S. Crozier, P. J. in 't Veld, A. Kohlmeyer, S. G. Moore, T. D. Nguyen, R. Shan, M. J. Stevens, J. Tranchida, C. Trott and S. J. Plimpton, *Comp. Phys. Comm.*, 2022, **271**, 108171.

[2]W. C. Swope, H. C. Andersen, P. H. Berens and K. R. Wilson, *J. Chem. Phys.*, 1982, **76**, 637–649.

[3]S. Nosé, *Mol Phys*, 2006, **52**, 255–268.

[4]M. Parrinello and A. Rahman, *J. Appl. Phys.*, 1981, **52**, 7182–7190.

[5]A. Haji-Akbari, R. S. DeFever, S. Sarupria and P. G. Debenedetti, *Phys. Chem. Chem. Phys.*, 2014, **16**, 25916–25927.

[6]Y. Lü, X. Zhang and M. Chen, *J. Phys. Chem. B*, 2013, **117**, 10241–10249.

[7]L. Martínez, R. Andrade, E. G. Birgin and J. M. Martínez, *J Comput Chem*, 2009, **30**, 2157–2164.

[8]N. Michaud-Agrawal, E. J. Denning, T. B. Woolf and O. Beckstein, *J Comput Chem*, 2011, **32**, 2319–2327.

[9]Richard J. Gowers, Max Linke, Jonathan Barnoud, Tyler J. E. Reddy, Manuel N. Melo, Sean L. Seyler, Jan Domański, David L. Dotson, Sébastien Buchoux, Ian M. Kenney and Oliver Beckstein, Proceedings of the 15th Python in Science Conference, 2016, pp. 98 – 105.

[10]R. W. Hockney and J. W. Eastwood, *Computer simulation using particles*, crc Press, 2021.

[11]J. Kolafa and J. W. Perram, *Mol Simul*, 1992, **9**, 351–368.

[12]T. Sayer and S. J. Cox, *Phys. Chem. Chem. Phys.*, 2019, **21**, 14546–14555.

[13]S. J. Cox and M. Sprik, *J. Chem. Phys.*, 2019, **151**, 064506.

[14]H. C. Andersen, *J. Comput. Phys.*, 1983, **52**, 24–34.

[15]A. Haji-Akbari and P. G. Debenedetti, *Proc. Natl. Acad. Sci. U.S.A.*, 2017, **114**, 3316–3321.

[16]R. H. Swendsen and J.-S. Wang, *Phys. Rev. Lett.*, 1986, **57**, 2607.

[17]D. J. Earl and M. W. Deem, *Phys. Chem. Chem. Phys.*, 2005, **7**, 3910–3916.

[18]M. B. Davies, M. Fitzner and A. Michaelides, *Proc. Natl. Acad. Sci. U.S.A.*, 2022, **119**, e2205347119.

[19]M. Bonomi, G. Bussi, C. Camilloni, G. A. Tribello, P. Banáš, A. Barducci, M. Bernetti, P. G. Bolhuis, S. Bottaro, D. Branduardi, R. Capelli, P. Carloni, M. Ceriotti, A. Cesari, H. Chen, W. Chen, F. Colizzi, S. De, M. D. L. Pierre, D. Donadio, V. Drobot, B. Ensing, A. L. Ferguson, M. Filizola, J. S. Fraser, H. Fu, P. Gasparotto, F. L. Gervasio, F. Giberti, A. Gil-Ley, T. Giorgino, G. T. Heller, G. M. Hocky, M. Iannuzzi, M. Invernizzi, K. E. Jelfs, A. Jussupow, E. Kirilin, A. Laio, V. Limongelli, K. Lindorff-Larsen, T. Löhr, F. Marinelli, L. Martin-Samos, M. Masetti, R. Meyer, A. Michaelides, C. Molteni, T. Morishita, M. Nava, C. Paissoni, E. Papaleo, M. Parrinello, J. Pfaendtner, P. Piaggi, G. M. Piccini, A. Pietropaolo, F. Pietrucci, S. Pipolo, D. Provasi, D. Quigley, P. Raiteri, S. Raniolo, J. Rydzewski, M. Salvalaglio, G. C. Sosso, V. Spiwok, J. Šponer, D. W. Swenson, P. Tiwary, O. Valsson, M. Vendruscolo, G. A. Voth and A. White, *Nat. Methods*, 2019, **16**, 670–673.

[20]G. A. Tribello, M. Bonomi, D. Branduardi, C. Camilloni and G. Bussi, *Comput Phys Commun*, 2014, **185**, 604–613.

[21]Cubic ice was also considered, and the corresponding distribution was found to be skewed to higher values of $P(\bar{Q}_6^{(i)})$. Since all systems are being seeded purely with hexagonal ice, we choose to base of derivation of $\bar{Q}_{6\mathrm{C}}$ on the liquid and Ih phases.

[22]E. Sanz, C. Vega, J. R. Espinosa, R. Caballero-Bernal, J. L. Abascal and C. Valeriani, *J. Am. Chem. Soc.*, 2013, **135**, 15008–15017.

[23]J. R. Espinosa, C. Vega, C. Valeriani and E. Sanz, *J. Chem. Phys.*, 2016, **144**, 034501.

[24]A. Haji-Akbari, *J. Chem. Phys.*, 2018, **149**, 072303.

[25]J. Russo, F. Romano and H. Tanaka, *Nat. Matter.*, 2014, **13**, 733–739.

[26]E. B. Moore and V. Molinero, *Nature*, 2011, **479**, 506–508.

[27]I. Sanchez-Burgos, A. R. Tejedor, C. Vega, M. M. Conde, E. Sanz, J. Ramirez and J. R. Espinosa, *J. Chem. Phys.*, 2022, **157**, 094503.